# SEMILEPTONIC AND ELECTROWEAK PENGUIN RESULTS FROM BABAR

JOHN WALSH [a]

(on behalf of the BaBar Collaboration)

*INFN, Sezione di Pisa, Largo Pontecorvo 3,*
*56127 Pisa, Italia*

We report recent results from the BaBar experiment on semileptonic charmless $B$-meson decays and electroweak penguin processes. Semileptonic charmless decays are used to determine $|V_{ub}|$ and the exclusive modes considered here also begin to constrain QCD-lattice form factor calculations. Radiative penguin decays are both sensitive to physics beyond the Standard Model and can be used to extract Heavy Quark parameters related to the $b$-quark mass and its motion inside the hadron.

## 1 Introduction

An important goal of the study of semileptonic charmless $B$-meson decays is the measurement of $|V_{ub}|$, which essentially measures one side of the Unitarity Triangle of the CKM matrix. Both inclusive and exclusive analyses have been used to measure $|V_{ub}|$, here we report on recent results using exclusive decays. The measurement of exclusive branching fractions is also useful for distinguishing among theoretical calculations of the form factors, as we shall see.

The the radiative decay $B \to X_s \gamma$ is studied as a probe of New Physics. Since this decay occurs at the one-loop level, the branching fraction is sensitive to models with additional heavy particles that can participate in the loop. In contrast, the shape of the photon energy spectrum is quite insensitive to contributions from New Physics, but it is rather sensitive to two important parameters of Heavy Quark (HQ) theory: the $b$-quark mass $m_b$ and the quantity $\mu_\pi^2$, which is related to the Fermi motion of the $b$-quark inside the hadron.

In this report, we present recent results from the BaBar experiment[1] on semileptonic charmless $B$-meson decays to exclusive states and on the $B \to X_s \gamma$ process. Beyond providing information on the CKM matrix and probing the possibility of New Physics, these analyses also provide insight into $B$-meson decay dynamics and QCD. All results presented herein are preliminary.

## 2 Exclusive semileptonic charmless $B$ decays

Semileptonic charmless $B$-meson decays to exclusive final states can be used to measure $|V_{ub}|$ by exploiting the dependence of the branching fraction on the CKM matrix element. In the case of $B^0 \to \pi^- \ell^+ \nu$, we have:

$$\frac{d\Gamma(B^0 \to \pi^- \ell^+ \nu)}{dq^2} = \frac{G_F^2}{24\pi^3}|V_{ub}|^2 p_\pi^3 |f_+(q^2)|^2 \qquad (1)$$

[a] john.walsh@pi.infn.it

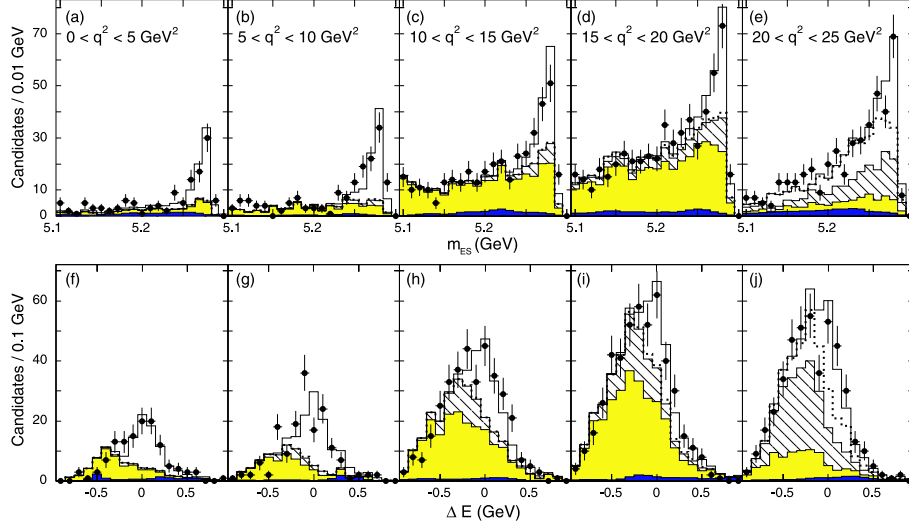Figure 1: Projected $m_{ES}$ (top) and $\Delta E$ (bottom) distributions in five bins of $q^2$ for the $B \to \pi\ell\nu$ modes. The data is represented by points with (statistical) error bars, while the simulation is shown as a histogram. The simulated components are: signal (white), combinatoric signal (dashed), crossfeed (hatched), $b \to c\ell\nu$ (light shaded) and continuum (dark shaded).

Here $G_F$ is the Fermi coupling constant, $p_\pi$ is the pion momentum in the center-of-mass frame, $q$ is the invariant mass of the lepton-neutrino pair and $f_+(q^2)$ is the form factor, which is calculated theoretically. The goal is to measure the branching fraction in bins of $q^2$, which allows one to distinguish among form factor calculations as well as extract the value of $|V_{ub}|$.

Experimentally, the branching fractions of exclusive $b \to u$ decays are small and backgrounds from $b \to c$ transitions are substantial. BaBar has used two different methods for overcoming the experimental difficulties: 1) an "untagged" analysis, based on 83 million $B\bar{B}$ pairs, where a premium is placed on high quality neutrino reconstruction using the missing momentum in the event; and 2) a "tagged" analysis (232 million $B\bar{B}$ pairs for the $B^0 \to \pi^-\ell^+\nu$ state, 88 million $B\bar{B}$ pairs for $B^+ \to \pi^0\ell^+\nu$ state), where backgrounds are reduced by requiring the other $B$-meson in the event be "tagged" via a $D^{(*)}\ell\nu$ decay.

The untagged analysis relies on good neutrino reconstruction to perform its measurement of the branching fractions of $B \to \pi\ell\nu$ and $B \to \rho\ell\nu$. The neutrino momentum is inferred from the event missing momentum and strict requirements are placed to ensure good neutrino reconstruction. For example, the event missing mass is required to be compatible with zero: since its resolution broadens linearly with missing energy, we require $|m_{\mathrm{miss}}^2/2E\mathrm{miss}| < 0.4$ GeV. The variables used to distinguish signal from background are $m_{\mathrm{ES}} = \sqrt{s/4 - |\vec{p}_B^*|^2}$ and $\Delta E = E_B^* - \sqrt{s}/2$, where $\sqrt{s}$ is the total energy in the $\Upsilon(4S)$ center-of-mass frame. Figure 1 shows the distribution of these two variables for the $B \to \pi\ell\nu$ modes in five bins of $q^2$. Branching fraction measurements from both the tagged and untagged analyses are reported in Table 1.

The statistics of the untagged sample permits the study of the $q^2$ dependence of the branching fraction and an investigation of several form factor calculations. Figure 2 shows the differential decay rates along with the predictions of four theoretical calculations: LCSR1 [2], LQCD1 [3], LQCD2 [4] and ISGW II [5]. The $\chi^2$ probabilities are good ($\sim 50\%$) for the first three calculations, while it is marginal (3%) for the ISGW II prediction. We extract the value of $|V_{ub}|$ using the $B \to \pi\ell\nu$ data and the LQCD2 calculation over the full $q^2$ range $0 - 25$ GeV$^2$. The BK parametrization [6] is used to extrapolate the LQCD2 form factor calculation to low $q^2$. We obtain $|V_{ub}| = (3.82 \pm 0.14 \pm 0.24 \pm 0.11^{+0.88}_{-0.52}) \times 10^{-3}$, where the uncertainties are due to statistics, systematics, form factor shape and form factor normalization, respectively.

Table 1: Branching fractions to charmless semileptonic exclusive states from the tagged (labeled "T") and untagged ("U") analyses. The uncertainties shown are statistical, systematic and (for the untagged analysis) due to form factor uncertainties. The untagged analysis assumes the isospin relations: $B(B^0 \to \pi^-(\rho^-)\ell^+\nu) = 2B(B^+ \to \pi^0(\rho^0)\ell^+\nu)$

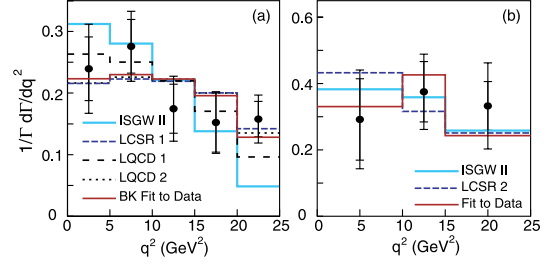| Mode (Technique) | Branching Fraction ($10^{-4}$) |
|---|---|
| $B^0 \to \pi^-\ell^+\nu$ (T) | $1.03 \pm 0.25 \pm 0.13$ |
| $B^+ \to \pi^0\ell^+\nu$ (T) | $1.80 \pm 0.37 \pm 0.23$ |
| $B^0 \to \pi^-\ell^+\nu$ (U) | $1.38 \pm 0.10 \pm 0.18 \pm 0.08$ |
| $B^0 \to \rho^-\ell^+\nu$ (U) | $2.14 \pm 0.21 \pm 0.53 \pm 0.28$ |

Figure 2: Comparison of the differential decay rate from the untagged analysis for $B \to \pi\ell\nu$ (left) and $B \to \rho\ell\nu$ (right) together with several theoretical form factor calculations.
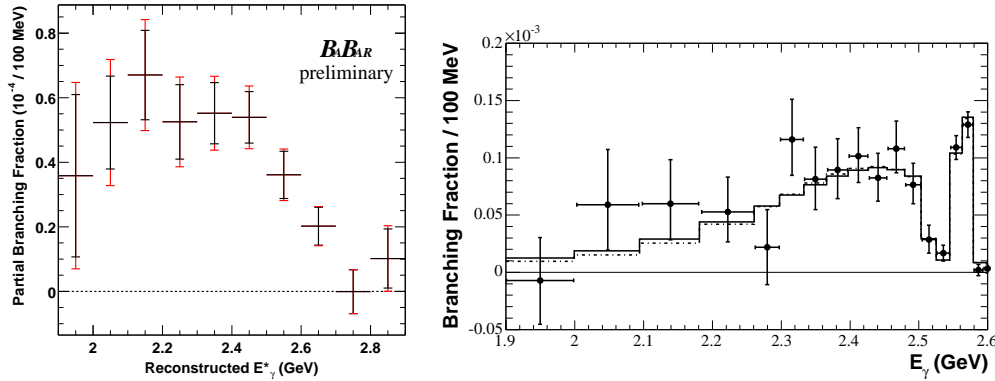


Figure 3: The photon energy spectrum, background-subtracted and efficiency-corrected, for the fully inclusive analysis (left) and the semi-inclusive analysis (right). The fully inclusive spectrum is measured in the $\Upsilon(4S)$ rest frame, while the semi-inclusive spectrum is measured in the $B$-meson rest frame. The peak due to $B \to K^*\gamma$ decays at high photon energy of the semi-inclusive spectrum is visible due to the good resolution (see text).

## 3   $B \to X_s\gamma$

BaBar has performed two analyses of the $B \to X_s\gamma$ channel: a fully inclusive measurement, where no requirements are made on the hadronic state ($X_s$) and a semi-inclusive analysis, which aims to reconstruct a large part of the total $B \to X_s\gamma$ rate by summing many exclusively reconstructed modes. The two approaches are complementary: the fully inclusive method requires a lepton tag to reduce continuum background, but nevertheless suffers from significant backgrounds from $B\bar{B}$ events. The semi-inclusive analysis, which sums 38 exclusive decay modes, has the advantage of reduced backgrounds due to the kinematic handles provided by fully reconstructed $B$ candidates. This analysis however, has a significant systematic uncertainty due to the *missing fraction*, the part of the $B \to X_s\gamma$ rate that it does not reconstruct. Both of these analysis are based on approximately 89 million $B\bar{B}$ pairs.

Figure 3 shows the resulting photon energy spectra for the two analyses. The semi-inclusive analysis has better photon energy resolution for two reasons: 1) the energy is measured in the $B$-meson rest frame and 2) the photon energy is actually inferred from the hadronic invariant mass, which has quite good resolution. We present in Table 3 the energy moments of the photon spectrum calculated above a certain energy threshold, measured in the $B$-meson rest frame. A correction is applied to the fully-inclusive values to bring them into this frame. These moments may be directly compared to theoretical calculations to give information on HQ parameters. A

Table 2: Photon energy spectrum moments and partial branching fractions (PBF) from $B \to X_s \gamma$. The first four rows are from the fully inclusive analysis, the remaining rows are from the semi-inclusive analysis. Values are given for the $B$-meson rest frame, including the minimum photon energy. The uncertainties shown are statistical, systematic and model-dependent (for the fully inclusive analysis), respectively.

| Min $E_\gamma$ | PBF $(10^{-4})$ | 1st Moment (GeV) | 2nd Moment $(GeV^2)$ | 3rd Moment $(GeV^3)$ |
|---|---|---|---|---|
| 1.9 | $3.67 \pm 0.29 \pm 0.34 \pm 0.29$ | $2.288 \pm 0.025 \pm 0.017 \pm 0.012$ | - | - |
| 2.0 | $3.41 \pm 0.27 \pm 0.29 \pm 0.23$ | $2.316 \pm 0.016 \pm 0.010 \pm 0.012$ | - | - |
| 2.1 | $2.97 \pm 0.24 \pm 0.25 \pm 0.17$ | $2.355 \pm 0.014 \pm 0.007 \pm 0.010$ | - | - |
| 2.2 | $2.42 \pm 0.21 \pm 0.20 \pm 0.13$ | $2.407 \pm 0.012 \pm 0.005 \pm 0.008$ | - | - |
| 1.897 | - | $2.321 \pm 0.044^{+0.037}_{-0.026}$ | $0.0253 \pm 0.0116^{+0.0049}_{-0.0042}$ | $0.0006 \pm 0.0085^{+0.0041}_{-0.0032}$ |
| 1.999 | - | $2.314 \pm 0.025^{+0.026}_{-0.027}$ | $0.0273 \pm 0.0039^{+0.0042}_{-0.0037}$ | $0.0009 \pm 0.0036^{+0.0036}_{-0.0022}$ |
| 2.094 | - | $2.357 \pm 0.018^{+0.014}_{-0.016}$ | $0.0183 \pm 0.0023^{+0.0021}_{-0.0012}$ | $0.0005 \pm 0.0017^{+0.0016}_{-0.0009}$ |
| 2.181 | - | $2.396 \pm 0.013^{+0.008}_{-0.004}$ | $0.0115 \pm 0.0014^{+0.0010}_{-0.0006}$ | $0.0001 \pm 0.0008^{+0.0006}_{-0.0003}$ |
| 2.261 | - | $2.425 \pm 0.009^{+0.004}_{-0.002}$ | $0.0075 \pm 0.0007^{+0.0003}_{-0.0002}$ | $-0.0001 \pm 0.0003^{+0.0002}_{-0.0001}$ |

fit to the semi-inclusive spectrum was performed to extract the HQ parameters $m_b$ and $\mu_\pi^2$. Two theoretical schemes were used to perform the fits: the kinetic scheme[7], which gives:

$$m_b = 4.69^{+0.05}_{-0.04} \text{ GeV} \quad \text{and} \quad \mu_\pi^2 = 0.30^{+0.07}_{-0.05} \text{ GeV}^2; \tag{2}$$

and the shape function scheme[8], which yields:

$$m_b = 4.65 \pm 0.04 \text{ GeV} \quad \text{and} \quad \mu_\pi^2 = 0.19^{+0.06}_{-0.05} \text{ GeV}^2; \tag{3}$$

where the errors are the sum of statistical and systematic, but do not include theoretical uncertainties. We note that the parameter $\mu_\pi^2$ is not defined the same way in the two schemes. The spectrum fit also yields the total inclusive branching fraction down to $E_\gamma > 1.6$ GeV. Averaging the results from the two theoretical schemes gives: $B(b \to s\gamma, E_\gamma > 1.6 \text{ GeV}) = (3.38 \pm 0.19^{+0.64+0.07}_{-0.41-0.08}) \times 10^{-4}$. We note that the branching fraction result is compatible with the Standard Model calculation[9] and with the experimental world average[10].

## Acknowledgments

## References

1. BaBar Collaboration, B. Aubert *et al.*, *Nucl. Instrum. Methods* A **479**, 1 (2002).
2. P. Ball, R. Zwicky, *Phys. Rev.* D **71**, 014015 (2005).
3. J. Shigemitsu *et al.* hep-lat/0408019.
4. M. Okamoto *et al.*, hep-lat/0409116; see also proceedings from this Conference.
5. D. Scora, N. Isgur, *Phys. Rev.* D **52**, 2783 (1999).
6. D. Becirevic, A.B. Kaidalov, *Phys. Lett.* B **478**, 417 (2000).
7. D. Benson, I.I. Bigi, N. Uraltsev, hep-ph/0410080.
8. M. Neubert, hep-ph/0412241.
9. P. Gambino, M. Misiak, *Nucl. Phys.* B **611**, 338 (2001); A.J. Buras, A. Czarnecki, M. Misiak, J. Urban, *Nucl. Phys.* B **631**, 219 (2002).
10. Heavy Flavor Averaging Group (HFAG), hep-ex/0412073.